Short communication

Neutron powder diffraction study of the influence of high oxygen pressure treatments on $La_2NiO_{4+\delta}$ and structural analysis of $La_2Ni_{1-x}Cu_xO_{4+\delta}$ $(0 \le x \le 1)$

A. Aguadero [a,*], M. Pérez [a], J.A. Alonso [b], L. Daza [a,c]

[a] *CIEMAT, Av. Complutense 22, E-28040 Madrid, Spain*
[b] *Instituto de Ciencia de Materiales de Madrid (CSIC), Campus Cantoblanco, E-28049 Madrid, Spain*
[c] *Instituto de Catálisis y Petroleoquímica (CSIC), Campus Cantoblanco, E-28049 Madrid, Spain*

Abstract

Materials formulated $La_2Ni_{1-x}Cu_xO_{4+\delta}$ $(0 \le x \le 1)$ have been prepared by the nitrate-citrate route, having an orthorhombic K_2NiF_4 structure with *Fmmm* ($x = 0$) and *Bmab* $(0.1 \le x \le 1)$ space groups. $La_2NiO_{4+\delta}$, which resulted to be the compound with the highest capability to accommodate excess oxygen ($\delta = 0.16$), underwent heat treatments (873–1098 K) under high oxygen pressure (200–250 bar). This led to an increase of excess oxygen in the structure. Rietveld refinements on neutron powder diffraction data probe the excess of oxygen to be accommodated as interstitial defect at the atomic position (1/4, 1/4, z; $z \approx 1/4$), which requires the displacement of four neighbouring oxygen atoms from their normal positions. This result is in agreement with a non-stoichiometry model which induces the stabilization of oxygen vacancies in the perovskite layer of these materials. The defect concentration determined from Rietveld refinement agrees well with the data obtained from thermogravimetric analysis. Results obtained herein reveal heat treatment under high oxygen pressure (873 K, 200 bar) as a promising method to enhance transport properties in K_2NiF_4-type structures.
© 2005 Elsevier B.V. All rights reserved.

Keywords: Neutron powder diffraction; Interstitial oxygen defect; K_2NiF_4 structures; Mixed conductors

1. Introduction

One of the main requirements to achieve the rapid commercialisation of the solid oxide fuel cell (SOFC) systems is the necessity to operate them at intermediate temperatures (550–850 °C) [1]. In this area mixed ionic electronic conductors (MIEC) are presented as a promising alternative to prepare cathodes as they decrease the overpotential of the oxygen reduction at the triple phase boundary (TPB), leading to a meaningful decrease of the operating temperature [2,3]. Other possible applications of MIEC concern membranes for oxygen purification or for partial oxidation of hydrocarbons as well as oxygen pumps and sensors [4,5].

Perovskite-like oxides have been the most widely studied as cathodes for SOFC applications, however these materials do not fulfil all the technological requirements for the adequate performance of SOFC systems [6,7]. This has led to an increasing interest in the search for new mixed conductors, where K_2NiF_4 structures have called considerable attention [8].

The crystal lattice of K_2NiF_4 structures can be described as a stacking of perovskite layers alternating with LaO rock salt layers. These compounds have shown to exhibit a wide range of oxygen hyperstoichiometry, which involves a considerable improvement of the transport properties [9–11].

The aim of this work is to study the mechanism of oxygen introduction in $La_2NiO_{4+\delta}$ by heat treatments under high oxygen pressure and to correlate it with the changes in its structure and transport properties. To fulfil this purpose neu-

---

* Corresponding author.
E-mail address: ainara.aguadero@ciemat.es (A. Aguadero).

tron powder diffraction technique was used. This technique is an extremely sensitive tool to detect, locate and quantify interstitial oxygen in the LaO layers of the structure.

2. Experimental

$La_2Ni_{1-x}Cu_xO_{4+\delta}$ powders ($0 \leq x \leq 1$) were prepared by the nitrate-citrate route. Stoichiometric amounts of analytical grade La_2O_3, CuO, $Ni(NO_3)_2 \cdot 6H_2O$ (Panreac) were dissolved in 8 M HNO_3 (Merck). Citric acid was then added to the mixtures in a molar ratio 3.3/1 with regard to $La_2Ni_{1-x}Cu_xO_{4+\delta}$. The resulting products were dehydrated before being calcined at 873 K for 30 min. Finally, they were fired in air at 1223 K for 8 h and slowly cooled down to room temperature.

The as-prepared powders underwent heat treatment (873–1098 K) under high oxygen pressure (200–250 bar) in a Morris Research furnace.

All compounds (before and after being treated) were characterized by X-ray diffraction (XRD) for phase identification and to assess phase purity. Analysis was performed in a Philips "X Pert-MPD" diffractometer using Cu Kα radiation ($\lambda = 1.5406$ Å). The diffraction patterns were recorded in the 2θ range 20–80° in steps of 0.04°.

Room temperature neutron powder diffraction (NPD) pattern of raw and O_2-treated $La_2NiO_{4+\delta}$ were collected in the high resolution D2B diffractometer at the ILL-Grenoble with a wavelength of 1.594 Å, selected from a Ge monochromator. The high flux mode was used. An amount of 3 g of each sample was contained in a vanadium can. The collection time was 2 h per pattern.

Diffraction data were analysed by the Rietveld method, using the FULLPROF program [12]. The line shape of the diffraction peaks was generated by a pseudo-Voigt function and the background refined to a 5th degree polynomial. In the final run the following parameters were refined: background coefficients, zero point, half width, pseudo-Voigt and asymmetry parameters for the peak shape, scale factor and unit cell parameters. Positional occupancy factors for oxygen atoms and isotropic thermal factors were also refined for NPD data.

The oxygen content in the powder samples was determined by thermogravimetric analysis in a TGA/SDTA851 Mettler Toledo thermobalance. Samples were heated in a flow
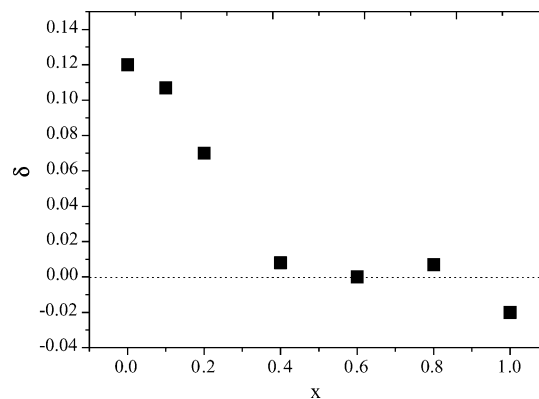

Fig. 1. Non-stoichiometric oxygen variation (δ) with copper content in $La_2Ni_{1-x}Cu_xO_{4+\delta}$ ($0 \leq x \leq 1$).

of 10% hydrogen (diluted in nitrogen) at 10 K min^{-1} up to 1273 K.

The cation contents of the powders were obtained by inductively coupled plasma-atomic emission spectroscopy (ICP-AES) using a Jobin Yvon equipment.

3. Results and discussion

The XRD patterns of the raw powders showed the existence of single orthorhombic K_2NiF_4-like phases for all compositions of the system $La_2Ni_{1-x}Cu_xO_{4+\delta}$ ($0 \leq x \leq 1$). Subsequent Rietveld refinement of the data displayed a *Bmab* space group for all the structures except for $La_2NiO_{4+\delta}$ (Table 1), which showed an *Fmmm* one. The unit-cell parameters a and b slightly decrease with the copper content, showing a very similar value in all cases except for a copper content of 1 mol per formula unit, where their values clearly differ, revealing an increase of the orthorhombic distortion. Parameter c regularly increases with the copper content. This is in agreement with the Jahn-Teller distortion induced by the introduction of Cu (II) with a d^9 configuration in the structure [13]. All these changes lead to an overall increase of the unit cell volume.

Thermogravimetric analysis on the powders showed a decrease of the oxygen excess (δ) with the copper content in the structures (Fig. 1). This could be due to the lower oxidation tendency of Cu (II) compared to Ni (II). ICP-AES data confirmed the cationic ratio to be as expected. Therefore, no lanthanum vacancies were created.

Table 1
Unit cell parameters for $La_2Ni_{1-x}Cu_xO_{4+\delta}$ system ($0 \leq x \leq 1$) refined in the *Fmmm* ($x = 0$) and *Bmab* ($0.1 \leq x \leq 1$) space groups from XRD data (raw samples)

| Sample	a (Å)	b (Å)	c (Å)	V (Å^3)
$La_2Ni O_{4+\delta}$	5.4629(5)	5.4612(5)	12.7039(1)	379.01(5)
$La_2Ni_{0.9}Cu_{0.1}O_{4+\delta}$	5.4565(2)	5.4508(2)	12.7403(1)	378.93(2)
$La_2Ni_{0.8}Cu_{0.2}O_{4+\delta}$	5.45369(8)	5.44428(8)	12.78887(9)	379.719(8)
$La_2Ni_{0.6}Cu_{0.4}O_{4+\delta}$	5.42474(9)	5.43055(9)	12.8843(2)	379.56(1)
$La_2Ni_{0.4}Cu_{0.6}O_{4+\delta}$	5.40850(4)	5.41132(4)	12.98266(4)	379.963(5)
$La_2Ni_{0.2}Cu_{0.8}O_{4+\delta}$	5.40147(3)	5.39196(4)	13.05317(7)	380.167(4)
$La_2CuO_{4+\delta}$	5.40244(3)	5.35539(3)	13.14435(7)	380.295(3)

Discrepancy factor: $R_{Bragg} = 6.8$–4.5%.
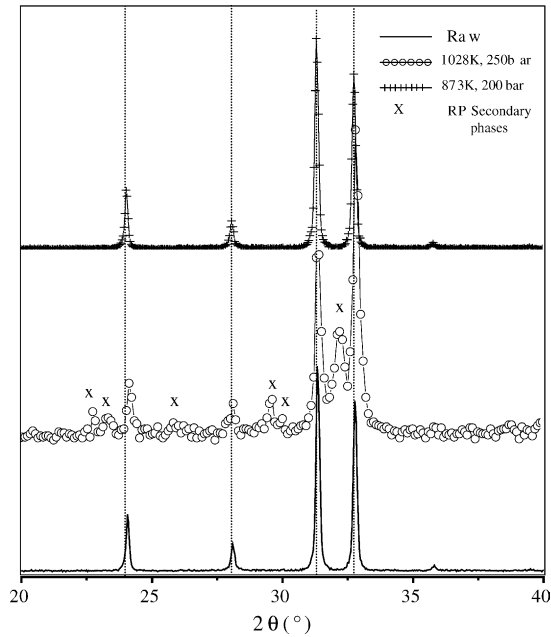
Fig. 2. XRD patterns for high oxygen pressure heat-treated $La_2NiO_{4+\delta}$ at (a) 1098 K, 250 bar and (b) 873 K, 200 bar.

Fig. 3. Observed (circles), calculated (full line) and difference (bottom) NPD Rietveld profiles at room temperature for $La_2NiO_{4+\delta}$ treated at 873 K, 200 bar. The series of tick marks corresponds to the allowed Bragg reflections.

Fig. 1 showed that $La_2NiO_{4+\delta}$ was the compound which more interstitial oxygen could accommodate in its structure. A first O_2-treatment at 1098 K and 250 bar was conducted. It led to the appearance of a secondary phase attributed to other members of the Ruddlesden-Popper family, $La_{n+1}Ni_nO_{3n+1}$, containing Ni cations in mixed 2+/3+ valence state. The formation of this unwanted phase was kinetically hindered by decreasing the reaction temperature down to 873 K [14]. The XRD pattern of the sample at this temperature shows the disappearance of the peaks associated to the secondary phase (Fig. 2).

Very useful information from the defect structure of the samples can be obtained from NPD data. Rietveld refinement of the crystal structure from these data makes possible to determine the interstitial oxygen positions and their occupancy factors with a quite good accuracy.

$La_2NiO_{4+\delta}$ has been reported to be tetragonal I4/*mmm* [15] or P42/*ncm* [16]; and orthorhombic *Fmmm* [17,18] or *Bmab* [18,19]. Although Jorgensen et al. attribute an orthorhombic *Fmmm* space group for compounds with $\delta < 0.13$ at room temperature, the Rietveld refinement of the structure of our raw samples ($\delta = 0.16$) initially revealed a better agreement with a *Bmab* one. However, an accurate analysis of the refinement data obtained for both space groups shows a great similarity between them. This led us to assume the one with the highest symmetry, *Fmmm*, as the most adequate space group. For this reason, the defect structure of $La_2NiO_{4+\delta}$ (before and after treatment) was successfully described by the model proposed by Jorgensen et al. [18]. This model proposes the introduction of interstitial oxygen at (1/4, 1/4, z; z ≈ 1/4) positions. The insertion of these additional oxygens into the lattice causes a displacement of O(2) from its normal position to O(4) posi-
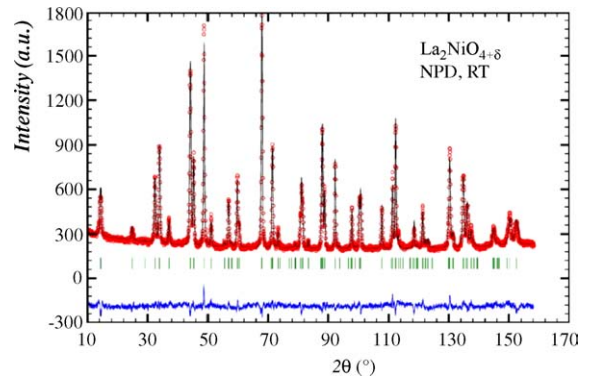
tion. This is indeed observed, since the refinement of oxygen site occupancies allows us to detect a large vacancy concentration at O(2) position. In accordance to this, occupancy of one O(3) defect would be expected to displace four neighbouring O(2) atoms into the O(4) site. Thus, the model is judged to be valid if $n(O(2)) + n(O(4)) \approx 2$ and $n(O(4)) \approx 4$ $n(O(3))$. This leads to $\delta_{(NPD)} \approx 2n(O(3))$, which is supported by the TG analysis of the samples. As shown in Fig. 3, an excellent fit between the observed and the calculated NPD profiles was obtained. Refinement parameters are given in Table 2. It is observed that the heat treatment under high oxygen pressure (873 K, 200 bar) involves an increase of the occupancy factor of O(3) sites in 0.026(1) ($\Delta\delta = 0.052$). This is accompanied by a decrease of the occupancy factor of O(2) positions. Therefore, the presence of interstitial sites favour the creation of oxygen vacancies (so-called Frenkel defects) [20,21], represented by:

$$O^xO(8e) \leftrightarrow V^{\bullet\bullet}_{O(8e)} + O_i''$$
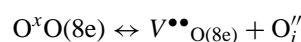
Additionally, the refinement of the isotropic thermal factors ($B (\text{Å}^2)$) reveals an enhancement of the mobility of O(2) and O(4) atoms. Thus, the treatment not only induces an increase of the number of defects in the structure but also an enhancement of their mobility.

Table 3 shows how interatomic distances are not greatly influenced by the treatment. A negligibly small decrease of the Ni–O(2) bond is observed, suggesting that no significant charge is transferred [22,23]. One possible explanation for this behaviour is that charge-neutral or O_i' defects are formed in the *Fmmm* phase. Most probably, the slight variation of non-stoichiometric oxygen between raw and O_2-treated $La_2NiO_{4+\delta}$ is not high enough to induce significant changes in the Ni–O(2) bond lengths, within the standard deviations. Other authors have attributed these defects to the presence of peroxide ions [24]. Nevertheless, the high volume of these species would involve the occupancy of two lattice positions (1/4, 1/4, z) and (1/4, 1/4, −z). This would require a value of $z < 0.2$, which is clearly not our case (see Table 2).

Table 2

NPD refined structural parameters for raw and O_2-treated (873 K, 200 bar) $La_2NiO_{4+\delta}$. Data were refined in the orthorhombic *Fmmm* space group

Parameter	Raw	Treated (873 K, 200 bar)
δ (TG)	0.16	0.20
a (Å)	5.45735(2)	5.45489(2)
b (Å)	5.46287(2)	5.46185(2)
c (Å)	12.69065(2)	12.70133(3)
V (Å^3)	378.344(2)	378.421(3)
La x	0	0
y	0	0
z	0.3604(1)	0.3600(2)
B (Å^2)	0.86(3)	0.86(3)
n	1	1
Ni $x=y=z$	0	0
B (Å^2)	0.80(3)	0.78(4)
n	0.5	0.5
O(1) $x=y$	1/4	1/4
z	0	0
B (Å^2)	0.96(3)	0.98(4)
n	1	1
O(2) x	0	0
y	0	0
z	0.1756(4)	0.1747(6)
B (Å^2)	1.4(1)	1.6(1)
n	0.68(2)	0.67(2)
O(3) $x=y$	1/4	1/4
z	0.25(5)	0.265(3)
B (Å^2)	1.0(6)	1.0(6)
n	0.090(6)	0.111(8)
O(4) x	−0.053(3)	−0.05(3)
y	−0.081(4)	−0.080(5)
z	0.171(1)	0.173(2)
B (Å^2)	1.4(1)	1.6(1)
n	0.37(2)	0.38(2)
R_{wp} (%)	12.4	14.0
χ^2	2.79	2.27

Table 3

Interatomic distances in raw and treated (873 K, 200 bar) $La_2NiO_{4+\delta}$ as determined from Rietveld refinement of NPD data

	Interatomic distance (Å)	
	Raw	Treated (873 K, 200 bar)
Host structure		
Ni—O(1)	1.9304(0)	1.9298(0)
Ni—O(2)	2.229(6)	2.219(7)
La—O(1)	2.620(1)	2.624(1)
La—O(2)	2.345(6)	2.353(7)
	2.7695(9)	2.766(1)
	2.7667(9)	2.763(1)
Defect structure		
Ni—O(4)	2.23(2)	2.26(2)
La—O(3)	2.4(4)	2.27(2)
	2.4(4)	2.50(3)
La—O(4)	2.46(2)	2.43(2)
	2.34(2)	2.35(3)
	2.51(2)	2.51(2)
O(3)–O(4)[a]	2.6 (2)	2.71(3)
	2.6(2)	2.40(3)

[a] In the case O(3)–O(4) only the long, physically meaningful distance is listed.

Finally, to the light of the results, we cannot assert which are the main charge carriers in the structure. It would be of high interest to carry out conductivity and permeation/diffusivity measurements on the system to clarify this aspect.

4. Conclusions

All compositions of the system $La_2Ni_{1−x}Cu_xO_{4+\delta}$ ($0 \leq x \leq 1$) prepared by the nitrate-citrate route herein showed the existence of single K_2NiF_4-like phases having an orthorhombic symmetry (*Fmmm* and *Bmab* space groups). The introduction of copper in the system decreases its capability to accommodate non-stoichiometric oxygen.

Heat treatment under high oxygen pressure (873 K, 200 bar) on $La_2NiO_{4+\delta}$ produces three main effects:

(a) an increase of non-stoichiometric oxygen in 0.05 mol per formula unit;
(b) an increase of oxygen vacancies concentration at O(2) sites of the lattice in 0.3 mol per formula unit;
(c) an enhancement of the mobility of interstitial oxygen located at O(2) and O(4) sites of the lattice from (B (Å^2)$_{raw}$ = 1.4 (1) to B (Å^2)$_{treate\,d}$ = 1.6 (1)).

As a consequence, the concentration of $V^{\bullet\bullet}_{O(8e)}$ is exalted by the O_i''. An increase in oxygen non-stoichiometry (δ) induces an increase in the number of $V^{\bullet\bullet}_{O(8e)}$ vacancies in the perovskite layer. This mechanism may explain, at least partly, the good efficiency of K_2NiF_4 structures when used as cathodes in solid oxide fuel cells devices. We can conclude that heat treatments under high oxygen pressure on these materials enhance this promising behaviour.

References

[1] A.B. Stambouli, E. Traversa, Renew. Sustain. Energy Rev. 6 (2002) 433–455.
[2] V.V. Kharton, A.P. Viskup, A.V. Kovalevsky, E.N. Naumovich, F.M.B. Marques, Solid State Ionics 143 (2001) 337–353.
[3] J. Fleig, J. Maier, J. Eur. Ceram. Soc. 24 (2004) 1343–1347.
[4] E. Boehm, J.M. Bassat, M.C. Steil, P. Dordor, F. Mauvy, J.C. Grenier, Solid-State Sci. 5 (2003) 973–981.
[5] A. Closset, S. Diethelm, K. Nisancioglu, J. Van Herle, A.J. McEvoy, J. Eur. Chem. Soc. 19 (1999) 843–846.
[6] E. Yvers-Yiffee, A. Weber, D. Herbstritt, J. Eur. Ceram. Soc. 21 (2001) 1505–1511.
[7] H. Ullmann, N.T.F. Tietz, D. Stover, A. Ahmad-Khanlou, Solid-State Ionics 21 (2000) 79–90.
[8] M.A. Daroukh, V.V. Vashook, H. Ullmann, F. Tietz, I.A. Raj, Solid-State Ionics 158 (2003) 141–150.
[9] V.V. Kharton, A.P. Viskup, E.N. Naumovich, F.M.B. Marques, J. Mater. Chem. 9 (1999) 2623–2629.
[10] S.J. Skinner, Solid-States Sci. 5 (2003) 419–426.
[11] A. Demourgues, A. Wattiaux, J.C. Grenier, M. Pouchard, J.L. Soubeyroux, J.M. Dance, P. Hagenmuller, J. Solid-State Chem. 105 (1993) 458–468.
[12] J. Rodriguez-Carvajal, Physica B 192 (1993) 55–69.

[13] A.R. West, Solid State Chemistry and its Applications, Wiley, 1987, pp. 310–311.

[14] M. Zinkevich, F. Aldinger, J. Alloys Compd. 375 (2004) 147–161.

[15] W. Paulus, A. Cousson, G. Dhalenne, J. Berthon, A. Revcolevschi, S. Hosoya, W. Treutmann, G. Heger, R. Le Toquin, Solid-State Sci. 4 (2002) 565–573.

[16] J. Rodríguez-Carvajal, M.T. Fernández-Diaz, J.L. Martínez, J. Phys.: Condensed Matter 3 (1991) 3215–3234.

[17] A. Demourgues, A. Wattiaux, J.C. Grenier, M. Pouchard, J. Solid-State Chem. 105 (1993) 458–468.

[18] J.D. Jorgensen, B. Dabrowski, S. Pei, D.R. Richards, D.G. Hinks, Phys. Rev. B 40 (1989) 2187–2199.

[19] M. Medarde, J. Rodríguez-Carvajal, Zeitschrift fuer Physik B 102 (1997) 307–315.

[20] J.M. Bassat, P. Odier, A. Villesuzanne, C. Marín, M. Pouchard, Solid-State Ionics 167 (2004) 341–347.

[21] L. Minervini, R.W. Kilner, K.E. Sickafus, J. Mater. Chem. 10 (2000) 2349–2354.

[22] G. Amow, P.S. Whitfield, I.J. Davidson, R.M. Hammond, C. Munnings, S. Skinner, Mater. Res. Symp. Proc. 755 (2003) 347–352.

[23] R.J. Cava, B. Batlogg, K.M. Rabe, E.A. Rietman, P.K. Gallagher, L.W. Rupp, Physica C 156 (1988) 523–527.

[24] D.J. Buttrey, P. Gamguly, J.M. Honig, C.N.R. Rao, R.R. Schartman, G.N. Subbanna, J. Solid-State Chem. 74 (1988) 233–238.